Chapter IV

Molecular Docking and MD simulation of human renin: implication on its binding site

4.1: Introduction

Renin is a hormone enzyme produced from the inactive protein prorenin [1]. Renin initiates renin-angiotensin system (RAS) producing the angiotensin peptides that control blood pressure, cell growth, apoptosis and electrolyte balanced [2-3]. Renin is highly specific aspartic proteinases and mainly produced by Juxtaglomerular cell in the kidney. The Secretion of renin from Juxtaglomrular cell is controlled by several mechanisms, including the sympathetic nervous system, salt and fluid balance, and blood pressure [4-7]. It cleaves angiotensinogen to form the decapeptide angiotensin I. Then inactive decapeptide converted to active octapeptide angiotensin II by the angiotensin converting enzyme (ACE). Next the angiotensin II binds to the type 1 angiotensin II receptors (AT1) [8]. Stimulation of type 1 angiotensin II receptor increases arterial tone and also the secretion of aldosterone. Therefore angiotensin II plays a key role in blood pressure, fluid and electrolyte homeostasis [9].

Inhibiting the renin-angiotensin system reduced stimulation of the AT1 receptor and thereby gives therapeutic benefits for the treatment of hypertension and congestive heart failure. Beta blockers are the original renin-angiotensin system inhibitor that inhibits the renin release from the kidney. Reduced renin secretion leads to decreased concentrations of angiotensinI and II. This is the benefits of beta blockade for protecting the heart from the heart attack [10]. Renin inhibitors are more efficient than ACE inhibitors and AT1 receptor antagonists. Renin inhibitors also have fewer side effects than the ACE inhibitors and AT1 receptor antagonists [11]. Renin is highly specific for only angiotensinogen. Therefore renin identified as an ideal target for antihypertensive drugs. The potent inhibitors of renin could give a new alternative way to treat high blood pressure without inhibiting other biological substances and thereby no side effects [12].

The design and development of renin inhibitors were started with peptidomemtic and it is specific for the angiotensinogen. The synthetic peptide inhibitors were not successful in treating hypertension as renin inhibitors due to the unfavorable pharmacokinetic behavior [13-16]. Therefore there was need new classes of nonpeptidic renin inhibitors that fulfill the criteria for becoming successful drugs. Now modern research has lead to the discovery of several classes of non-peptidic renin inhibitors. Aliskiren is the first marketed non-peptidic renin inhibitor [17, 18].

The human renin contains 340 amino acids. Structurally renin consist two homologous lobes with an active site at interface [13, 18]. The catalytic activity of the active site is due to two aspartic acid residues (Asp38, Asp226), one located in each lobe of the renin molecule. The active site of renin can accommodate seven amino acid residues of angiotensinogen and cleaves the Leu10-val11 peptide bond within angiotensinogen to generate angiotensin I [19].

In this study MD simulation was performed to consider the flexibility of protein. Molecular docking studies were employed to determine the binding mode of renin and its inhibitor.

4.2: Materials and Methods

Computational details

Preparation of protein

In the present article crystallographic structure of Human renin in complex with ligand 72X was obtained from Protein Data Bank (PDB code 3GW5), which have 669 residues with two chains (A and B) [20]. Missing atoms were repaired by the SPDBV software package [21]. We have removed all ligands from protein to get the free protein. For

docking simulation using Autodock all polar hydrogen was added with the GROMACS modeling package. The resulting structure was optimized 54 steps of conjugate gradient minimization, employing the GROMACS force field. During minimization, the heavy atoms were kept fixed at their initial crystal coordinates by restraing. Minimization was carried out under a vacuum medium. Electrostatic interactions were calculated using the cut-off method. Finally, solvation parameters were added using the ADDSOL utility of AutoDock 4.2. Default values of atomic solvation parameters were used throughout the calculations. The grid maps of the protein were used in the docking experiments was calculated using the AutoGrid utility program.

Preparation of inhibitor

Piperidine derivative 72X of renin inhibitor was collected from Protein Data Bank. Structure of renin inhibitor 72X is represented in Figure 1. For docking experiments with AutoDock 4.2, ligand molecule was optimized, and saved as in pdb format with the aid of Arguslab 4.2. Next ligand is loaded in AutoDock Tool (ADT). Gasteiger charges are added and 43 non polar hydrogens are merged. ADT also detected 15 rotatable bonds and 13 numbers of torsional degrees of freedom (TORSDOF). ADT selected a root with the minimum number of rotatable branches. Root was detected. Next ligand was saved in PDBQT format. Then prepared ligand was used in docking simulation in the next step.

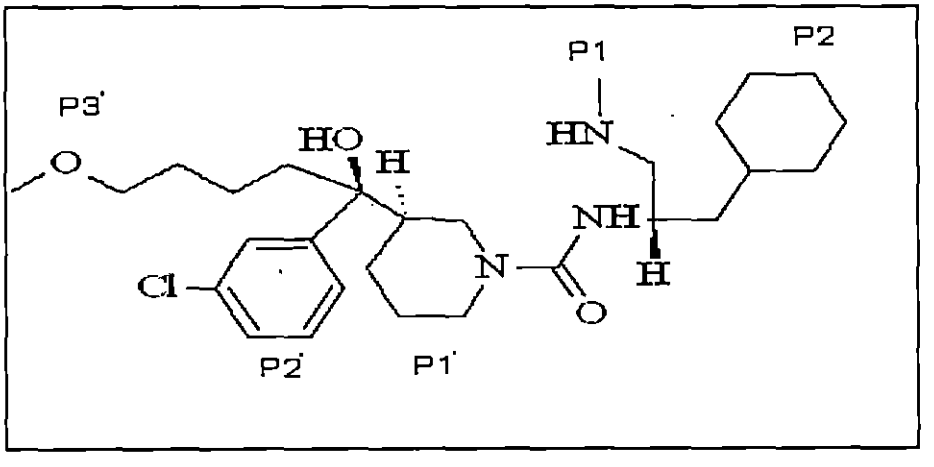

Fig 1: Structural representation of renin inhibitor 72X.

The piperidine and Teoc derivatives attached by amide linkage (at the P1-P1' position) in Renin inhibitor 72X [20]. We have divided the molecule in several moieties. P1' residue of 72X is a Piperidine moiety. The P2' residue of the renin inhibitor is a Chlorobenzene moiety. Similarly P3', P1, P2 residues are Methoxy butyl, (methyl amine) methyl, cyclohexyl moieties respectively.

We have listed the binding site residues of 72X from pdb and cross checked it by taking the residues within 3.5 Å from the inhibitor 72X. We selected 18 residues whose RMSD and Docking simulation have been performed. Each of these residues selected as a flexible residue in Autodock to evaluate the flexible docking.

MD Simulation

The MD simulation was carried out using GROMACS [24]. The 2.00 A° resolution x-ray structure of Human renin (PDB code 3GW5) was used as a starting structure. We have carried out MD simulation of free protein not the complex. The protein was solvated with SPC water molecules in a cubic box, having an edge length of 3.5 A°. The LINCS algorithm was employed to constrain all bond lengths (25). The simulation was conducted at a constant temperature (300K) and the Berendsen coupling method was used for coupling each component separately to a temperature bath [26]. To calculate longer-rang electrostatic contribution on a grid with spacing and a cutoff of 1.0 nm for Coulomb interaction we employed Lennard Jones interaction and the particle mesh Ewald method. MD simulation was performed for 6 ns. Before running simulation, an energy minimization was performed by steepest descent (sd) method. After that the positional

restraints were released and simulation is performed for 6ns with time step 2 fs. Finally the end of the simulation the respective trajectory files were examined with different tools of GROMACS.

Docking

Molecular docking studies were performed with AutoDock 4.2 using a Lamarckian genetic algorithm (LGA) to evaluate the inhibitor–enzyme interactions [27]. A grid map with 62 x 66 x 62 Å points with a grid spacing of 0.375 Å was generated using AutoGrid 4.2 and the grid was centered at x, y, z coordinates of 95.848, 108.694, 107.689. The distance dependent function of the dielectric constant was used for the calculation of the energy map. At the end of the docking experiment we get 10 dock conformers with different free energy of binding. The best conformer was chosen based on the lowest free energy of binding. The protein with the best conformer is saved as complex and analyzed using Molegro Molecular Viewer [28].

4.3: Results and Discussion

The overall structural stability of the free protein during the simulation has been monitored using several parameters likes the radius of gyration (Rg), RMSF and RMSD of individual residues were calculated over the course of the simulation.

The variation of radius of gyration (Rg) as a function of time is presented in Figure 2 and from this figure it is clear that the initial Rg value is 2.68172 and then Rg value decreases up to 437pswith Rg value 2.6126, after that Rg slightly increases up to 5261ps(2.69299). The overall plot of Rg during the simulation shows a periodical nature.

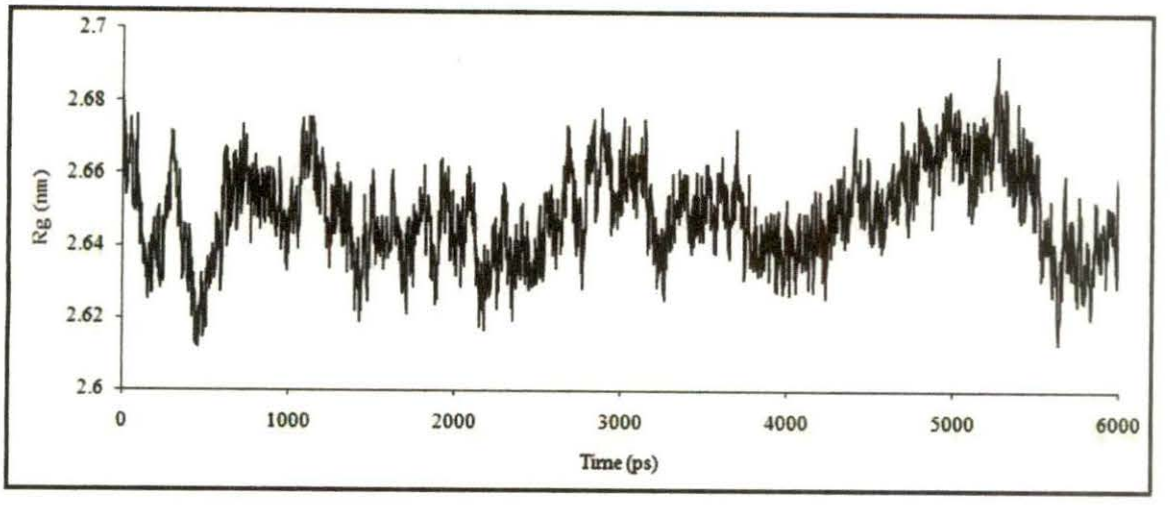

Fig. (2). Radius of gyration (Rg) as a function of time with respect to starting structure during the MD simulations is shown for human renin.

The flexibility of different segments of the protein is also revealed by looking at the root mean-square fluctuation (RMSF) of each residue from its time-averaged position is presented in Figure3.

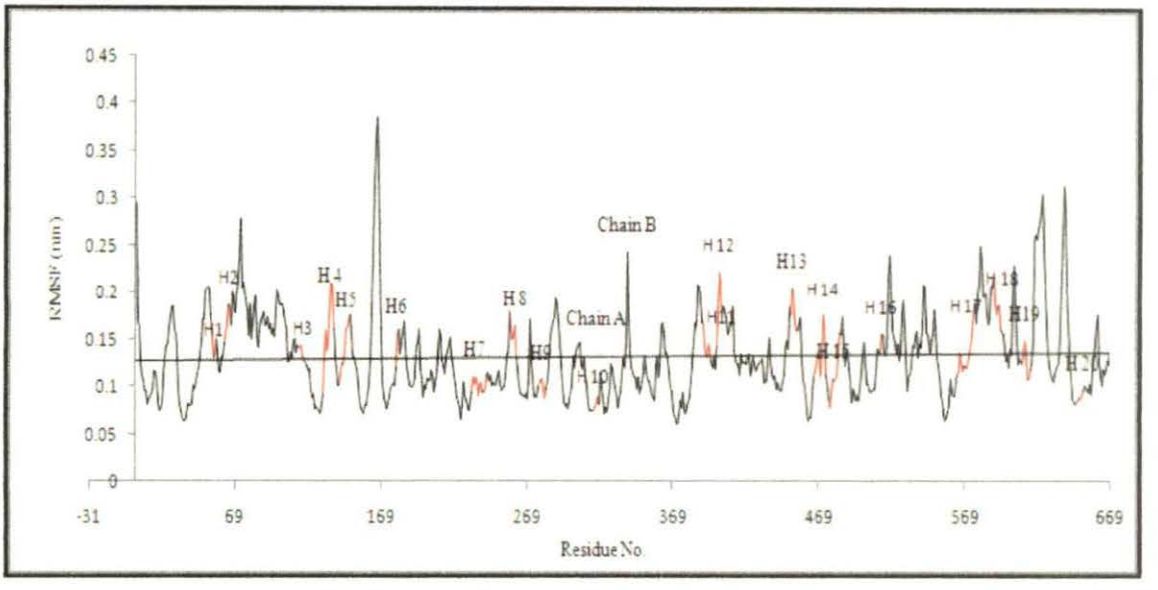

Helix(H) of Chain A	Residue No. in pdb	Residue No. after MD
H1	55-59	52-56
H2	65-69	62-66

Helix(H) of Chain B	Residue No. pdb	Residue No. after MD
H11	56-61	390-395
H12	65-69	399-403

Helix(H) of Chain A	Residue No. in pdb	Residue No. after MD
H3	11120	112-117
H4	132-140	129-137
H5	142-151	139-148
H6	182-184	179-181
H7	234-247	231-244
H8	260-265	257-262
H9	280-285	277-282
H10	316-321	313-318

Helix(H) of Chain B	Residue No. pdb	Residue No. after MD
H13	115-120	449-454
H14	132-140	466-474
H15	142-150	476-484
H16	182-184	511-513
H17	235-247	564-576
H18	260-265	589-584
H19	280-285	609-614
H20	316-321	645-650

Fig. (3). Root mean square fluctuations (RMSF) during the MD simulations are shown for human renin.

Among the secondary structure beta strand has higher fluctuation than alphahelix. There is ten Helix in both chains (A&B) within the protein in which Helix, H2 in chain B has highest fluctuations and Helix H10 in chain A has lowest fluctuations. Heilix H2, H4, H6 and H8, in chain A and H13, H14, H16, H17and H18 in chain B shows considerable fluctuations.

To understand the fluctuation of binding site residues of protein, RMSD of each residue was calculated. The average RMSD and their corresponding standard deviation (SD) for the residues are represented in a histogram (Figure 4).

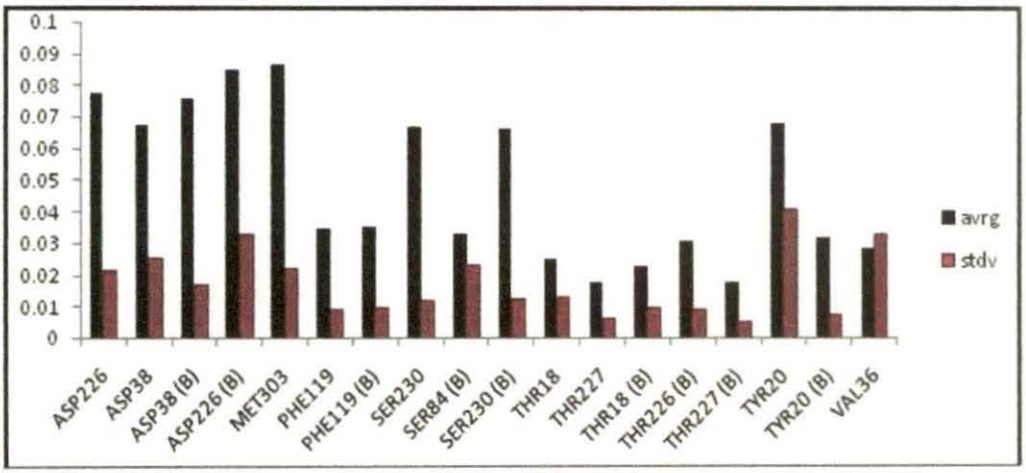

Fig. (4). Average RMSD and their corresponding standard deviation (SD amino acid residues

From the histogram it is examined that Thr227 shows the lowest fluctuation. Also Thr 227 (B), Thr18 and Val36 have low fluctuation. It is observed that Ser230 has low fluctuation than Met303.

To get insight about the binding mechanism, the residues of binding site were critically analyzed. The residues THR18, VAL36, THR227, SER230 and ASP38 (B) are very important for binding processes. From the RMSD values during the simulation time it is evident that the residues Thr227, Thr18 and Ser230 have very low fluctuation, as shown in Figure 5.

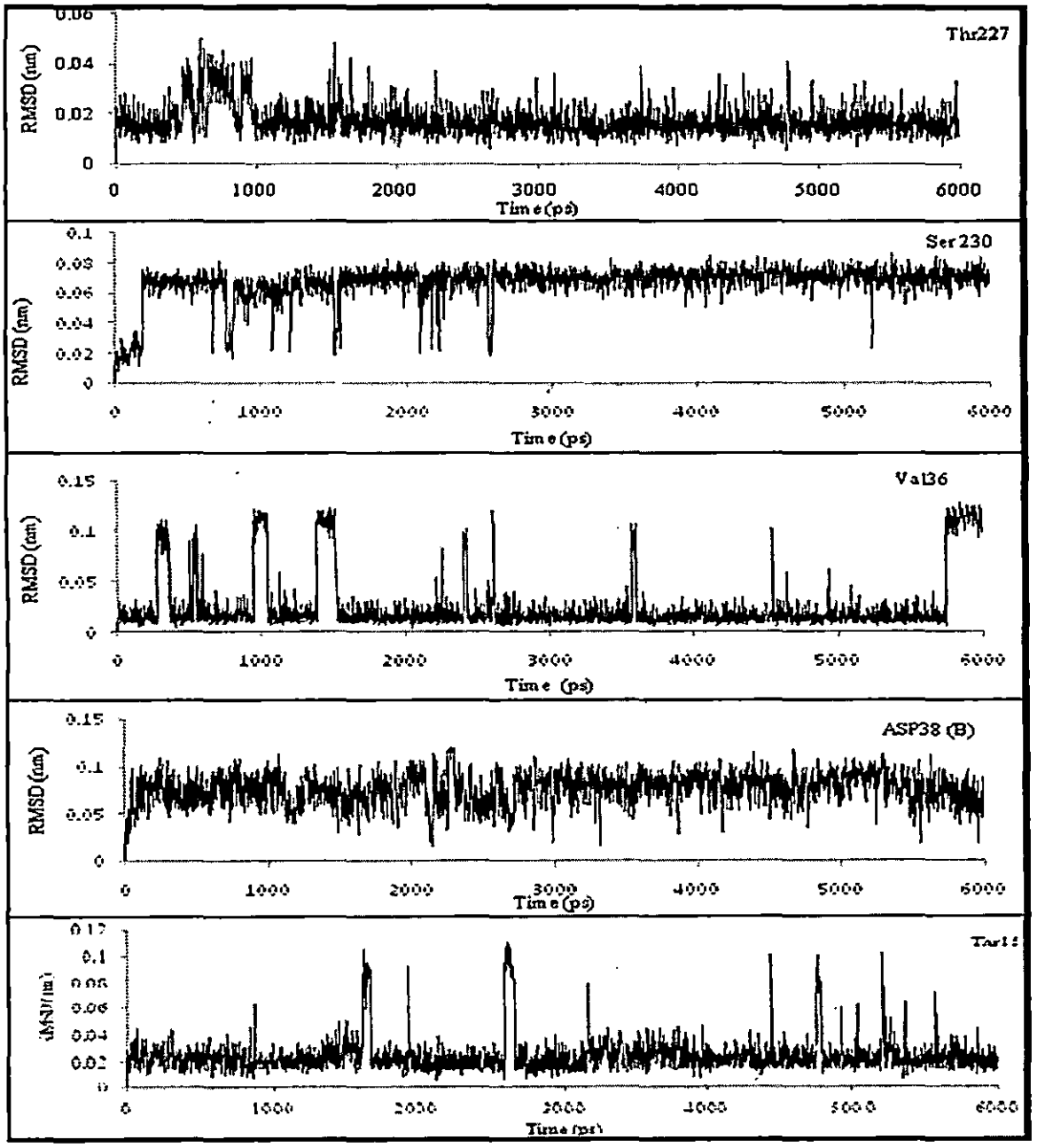

Fig. (5). RMSD: Root mean square deviations (RMSD) of the Thr227, Ser 230, Val36, Asp38 (B), Thr18 as a function of time with respect to starting structure during the MD simulations.

The residues Val36, Asp38 (B) have high fluctuation, and the fluctuation was moderate for the residues during the whole simulation time.

Now we have performed the docking simulation using those binding residues whose RMSD values have been already calculated. The residues having different fluctuation are

taken as flexible residue to see the effect of fluctuation in docking study. Each one of these residue selected as a flexible part to evaluate the flexible docking. Therefore we get 18 dock results and their corresponding binding energies are listed in Table 1.

Table 1.The free energies of binding of 72X with different residues selected as a flexible residue calculated by AutoDock 4.2

Docking No	Residue	Binding Energy (kcal/mol)
12	THR227	-9.66
8	SER230	-9.53
18	VAL36	-9.34
3	ASP38 (B)	-9.05
11	THR18	-8.96
5	MET303	-8.82
16	TYR20	-8.8
9	SER84 (B)	-8.71
6	PHE119	-8.48
1	ASP226	-8.07
2	ASP38	-8.07
15	THR227 (B)	-7.87
10	SER230 (B)	-7.8
13	THR18 (B)	-7.39
7	PHE119 (B)	-7.07
4	ASP226 (B)	-6.59
14	THR85 (B)	-6.43
17	TYR20 (B)	-5.49

From the table1 it is clearly shown that the docking with chain A residues as a flexible part have low binding energy. Low binding energy (-ve sign) indicates favorable binding (only a negative ΔG value is energetically favorable). Lowest binding energy value is obtained for Thr227 and. But docking with the chain B residues has moderately high

binding energy except Asp 38 (B) and Ser 84 (B). It is revealed from the RMSD binding energy data that low fluctuated residues have low binding energy. From table1 we choose five residues such as Thr227, Ser227, Val36, Asp38 (B) and Thr18. Each of them is favorably bound with inhibitor and RMSD is found lowest for Thr224 among the five residues.

Inhibitor 72X was successfully docked into the active site of human renin and calculated free energy of binding is shown in table1. From the table1 it is clear that the lowest binding energy value is obtained for Thr227 and docking with chain A residues as flexible part have low docking energy than the chain B residues except Asp 38 (B) and Ser 84 (B).

Docking structures are shown in Figure 6. The hydroxyl oxygen atom of the renin inhibitor was placed to make the hydrogen bond to an amide group of Ser230 (Figure 6A). The same hydroxyl oxygen atom makes a hydrogen bond with a side chain hydroxyl group of Ser230. The amino hydrogen atom of P1 moiety forms a hydrogen bond with the main chain carbonyl oxygen atom of Asp38. The hydroxyl hydrogen atom of the inhibitor is hydrogen bonded to an oxygen atom of the amide group of Gly228. The oxygen atom of P3' moiety forms a hydrogen bond with an amide group of Tyr20. A care full inspection of the binding pocket indicated that 72X adopt a position surrounded by hydrophobic groups Met303, Leu252, Thr85, Thr227, Phe124, Tyr231, Thr18, and Tyr20.

Figure 6B shows the four hydrogen bond interaction observed between inhibitor and human renin. The hydroxyl oxygen atom of inhibitor makes a hydrogen bond with the side chain hydroxyl group of Ser230. The same oxygen atom forms two hydrogen bonds with amide hydrogen of Ser230 and the carbonyl oxygen of Gly228. The fourth hydrogen bonding interaction observed between the oxygen atom of P3'moiety and amide

group of Tyr20. Inhibitor occupied a position in a hydrophobic cage surrounded by Leu121, Val127, Thr85, Thr18, Tyr20 and Ala229.

In Figure 6c, we examined three hydrogen bonds between 72X and Asp226, Gly228, Ser230. The amino hydrogen atom of P1 moiety makes a hydrogen bond with a side chain oxygen atom of Asp226. The hydrogen atom of the amide group of inhibitor forms a hydrogen bond with the amide oxygen of Gly228. Third hydrogen bonding involves between hydroxyl group of an inhibitor and side chain oxygen atom of Ser230. 72X make a position surrounded by hydrophobic residues Tyr20, Val36, Thr85, Leu221, Thr227 and Ala229.

Figure 6D shows three hydrogen bonds are formed between 72X and Asp226, Gly228, Ser230. It is observed that the hydrogen bonding interactions similar to the previous docking experiment (Figure 6C) 72X was surrounded by hydrophobic residues, such as Tyr20, Thr18, Met303, Tyr83 and Pro115.

The entire Figure 6A-Figure 6D imply that the P1 and P3' moieties hold large number of residues and their binding energies are low i.e. favorable binding. But the docking result in Figure 6E shows P1 moiety to have two nearest amino acid residues and P3' moiety have only one. Therefore docking for residue Tyr20 (B) as a flexible part in chain B binding energy is high. The hydroxyl hydrogen atom of inhibitor forms a hydrogen bond with a side chain oxygen atom of carboxylic acid group of Ser230. Second hydrogen bond forms between hydroxyl group of 72X and main chain carbonyl oxygen atom of Gly228. Another hydrogen bond forms between methyl amino group and main chain carbonyl group of Asp226. 72X surrounded by hydrophobic residues Phe 20 (B), Met303, Tyr83, Val 127, Ala226, Ala229 and Tyr23.

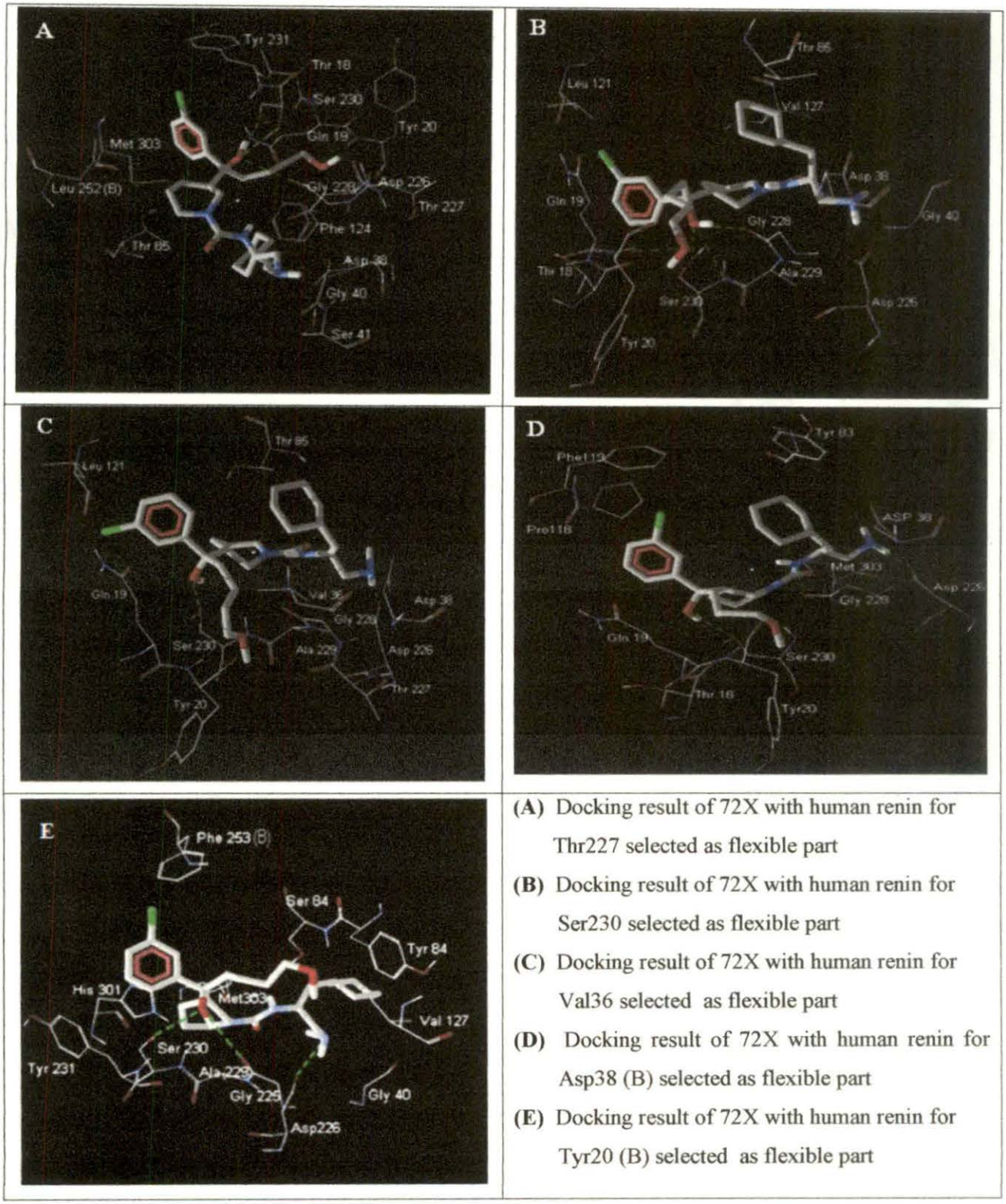

(A) Docking result of 72X with human renin for Thr227 selected as flexible part

(B) Docking result of 72X with human renin for Ser230 selected as flexible part

(C) Docking result of 72X with human renin for Val36 selected as flexible part

(D) Docking result of 72X with human renin for Asp38 (B) selected as flexible part

(E) Docking result of 72X with human renin for Tyr20 (B) selected as flexible part

Fig. (6). Docking results of 72X with a human renin for the Thr227, Ser230, Val (36), Asp38 (B), Tyr20 (B) selected as flexible part. The inhibitor 72x is presented by stick model and the residues in the active site of human renin are presented by wire frame.

Table 2 shows the free energies of binding of 72X with different residues selected as a flexible residue and their binding site residues

Table 2.The free energies of binding of 72X with different residues selected as flexible residue calculated by AutoDock 4.2

Residue	Binding energy (kcal/mol)	Binding site residues
Thr227	-9.66	Asp226, Asp38, Gln19, Gly228, Gly40, Leu252(B), Met303, Phe124, Ser230, Ser41, Thr18, Thr227, Thr85, Tyr 231, Tyr20
Ser230	-9.53	Ala229, Asp226, Asp38, Gln19, Gly228, Gly40, Leu121, Ser230, Thr18, Thr85, Tyr20, Val127,
Val36	-9.34	Ala229, Asp226, Asp38, Gly19, Gly228, Leu121, Ser230, Thr227, Thr85, Tyr20 Val36,
Asp38 (B)	-9.05	Asp226, Asp38, Gln19, Gly228, Met303, Phe119, Pro118, Ser230, Thr18, Tyr20, Tyr83
Tyr20 (B)	-5.49	Ala229, Asp226, Gly228, Gly40, His301, Met303, Phe253 (B), Ser230, Ser84, Tyr231, Tyr83, Val127

Renin inhibitor 72X possesses a hydrophobic environment surrounded with P1, P2, P1', P2' and P3' residues. LogP value (4.59) suggests hydrophobicity of the inhibitor is quite high [29]. Thus the hydrophobic interaction is important for stabilizing the complex. Interactions of inhibitor moieties with the active site residues of human renin at 3.5 Å are shown in table 3.

Table 3. Interactions of inhibitor moieties with the active site residues of human renin at 3.5 Å.

Residue	P1	P2	P1'	P2'	P3'
Thr 227	Asp38, Asp226 Gly 40, Ser 41	Phe 124	Thr85, Leu252(B), Met303	Tyr231	Gln19, Gly228, Thr 18, Tyr20, Thr227
Ser 230	Asp38, Asp226, Ala 229, Gln40	Val127,	Thr85	Leu121 Gln19	Thr18, Tyr20, Gly228
Val36	Asp38, Asp226,	Thr85		Leu121, Gln19	Tyr 20, Thr227, Ala229, Gly228
Asp38 (B)	Asp226	Tyr83, Asp38		Pro118, Phe119	Gly228, Ser230, Tyr20, Gln19, Thr18
Tyr20 (B)	Asp226, Gly40	Ser84, Tyr83	His301, Ala229, Tyr231, Ser230	Phe253(B)	Val127,

Figure 6A shows highly hydrophobic P2 moiety of 72X is closest to the hydrophobic phenyl ring of Phe124 at about 3.5 Å. Piperidine ring of inhibitor accommodates hydrophobic pocket formed by the residues Met303, Leu252 (B), and Thr85. Also P3' moiety forms hydrophobic contacts with the Thr 18, Tyr 20, Thr227, Gln19 and Gly228. Within 3.5 Å, P1 moiety accommodates feebly hydrophobic region. P2' moiety forms hydrophobic contacts with phenyl ring of the Tyr 231. From the Figure 6B it is seen that P2-cyclohexyl residue closer to hydrophobic residue Val127. P1' residue close to Thr85. P3' moiety accommodates the hydrophobic residues Thr18, Tyr20 and Gly228. P2'

moiety is closer to Leu121, Gln19. Figure 6C shows, Thr85 and cyclohexane ring of the inhibitor close to each other. P2' moiety of the inhibitor exists in close proximity to Leu121 and Gln19. Strong hydrophobic interactions observed between P3' moiety and each of the Tyr20, Thr224, Ala229, Gly228. In Figure 6D, P3'-metoxy butane moiety placed in the hydrophobic pocket surrounded by hydrophobic residues, such asTyr20, Thr18, Gly228, Ser230 and Gln19. Figure 6E shows Val 127 closer to methoxy butane moiety. Fewer number of hydrophobic amino acid residues are surrounded the hydrophobic part of the inhibitor. All the docking result shows two aspartic acid residues Asp38 and Asp226 placed at the P1 moeity. The chlorobenzene, cyclohexyl and methoxy butyl moieties of 72X fragments in a hydrophobic pocket composed amino acid residues Phe119, Phe124, Val127 and Tyr83. Each and every one docking result shows that inhibitor in hydrophobic cage surrounded by largely hydrophobic residues of renin. From Figure 6A-Figure 6D it is seen that hydroxyl group, P3', P1 moiety lie in approximately same side in 72X but Figure 6E shows P3' moiety is distorted. Maximum numbers of residues interact with 72X at that region. Opposite side has less number of residues that interact with the inhibitor. We have obtained different lowest free energy conformers from the docking experiment and it is observed that they have large conformational change. These conformational changes may differentiate the binding affinity of the amino acid residues around the inhibitor. Figure 6A-Figure 6B shows maximum number residues in chain A are involved in the binding process whereas only two residues Leu252 (B) and Phe253 (B) of chain B are involved in the binding process.

Docked conformer with lowest binding energy value is superimposed with the ligand from crystallographic structure of the complex, using the Accelrys Discovery Studio 2.5 and RMSD was obtained 2.12 Å. It is presented in Figure 7.

Fig. (7). Superimposition of the ligand from crystallographic structure of the complex with docked conformer of 72X. Ligand from crystallographic structure is shown in green and docked conformer in red.

4.4: References

1. Danser AHJ, Denium J (2005) Renin, pro-renin and the putative (Pro) renin receptor. *Hypertension*, **46**: 1069–1076.

2. Laragh JH (1960)The role of aldosterone in man: Evidence for regulation of electrolyte balance and arterial pressure by renaladrenal system which may be involved in malignant hypertension. *J.A.M.A.*, **174**: 293-295.

3. Ames RP, Borkowski AJ, Sicinski AM, Laragh JH (1965) Prolonged infusions of angiotensin II and norepinephrine and blood pressure, electrolyte balance,

aldosterone and cortisol secretion in normal man and in cirrhosis with asrites. *J. Clin. Invest.*,**44**: 1171-118.

4. Laragh JH, Baer L, Brunner HR, Buhler FR, Vaughan JE (1972) Renin, angiotensin and aldosterone system in pathogenesis and management of hypertensive vascular disease. *Am. J. Med.*, **52**: 633-652.

5. Chen KS, Tang J (1972) Amino acid sequence around the epoxide-reactive residues in pepsin. *J. Biol. Chem.*, **247**: 2566-2574.

6. Hartsuck JA, Tang J (1972)The carboxylate ion in the active centre of pepsin. *J. Biol. Chem.*, **247**: 2575-2580.

7. Reudelhuber, T.L.; Ramla, D.; Chiu, L.; Mercure, C.; Seidah, N.G. Proteolytic processing of human pro-renin in renal and non-renal tissues. *Kidney Int.*, **1994**, 46, 1522–1524.

8. Kaschina E, UngerT (2003) Angiotensin AT1/AT2 receptors: regulation, signalling and function. *Blood Press.*,**12**, 70–88.

9. Kim, S.; Iwao, H. Molecular and cellular mechanisms of angiotensin II-mediated cardiovascular and renal diseases. *Pharmacological reviews*, **2000**, 52 (1), 11-34.

10. Campbell DJ, Aggarwal A, Esler M, Kaye D (2001) Beta-blockers, angiotensin II, and ACE inhibitors in patients with heart failure. *Lancet.* **358:** 1609-10.

11. Stanton A (2003) Therapeutic potential of renin inhibitors in the management of cardiovascular disorders. *American Journal of cardiovascular drugs*, **3**: 389-394.

12. Norman KH (*2005*) Therapeutic opportunities for renin inhibitors, *J.R.A.A.S.*, **1**, 107–109.

13. Rahuel J, Rasetti V, , Maibaum J, Rüeger H, Göschke R, et al. (2000) MG. Structure-based drug design: the discovery of novel nonpeptide orally active inhibitors of human renin. *Chemistry & biology*, **7**: 493-504.

14. Fisher ND, Hollenberg NK (2001) Is there a future for renin inhibitors?.*Expert. Opin. Investig. Drugs*, **10**: 417–426.

15. Wood JM, Maibaum J, Rahuel J, Grutter MG, Cohen NC, et al. (2003) Structure-based design of aliskiren, a novel orally effective renin inhibitor. *Biochem. Biophys. Res. Commun.*, **308**: 698-705.

16. Rongen GA, Lenders JW, Smits P, Thien T (1995) Clinical pharmacokinetics and efficacy of renin inhibitors. *Clinical Pharmacokinetics*,**29**: 6–14.

17. Cohen NC (2007) Structure based Drug design and the discovery of aliskarin (Tekturna): Perseverance and creativity to overcome a R&D pipeline challenged. *Chemical Biology & Drug Design*, **70**: 557-565.

18. Gradman AH, Kad R (2008) Renin Inhibition in Hypertension. *J. Am. Coll. Cardiol.*, **51**: 519-528.

19. SieleckiAR,Hayakawa K, FujinagaM, MurphyME, Fraser M, et al. (1989)Structure of recombinant human renin, a target for cardiovascular-active drugs, at 2.5Å resolution. *Science*, 243: 1346-1351.

20. Ticea CM, Xua Z, Yuana J, Simpsona RD, Cacatiana ST,et al. (2009) Design and optimization of renin inhibitors: Orally bioavailable alkyl amines. *Bioorganic & Medicinal Chemistry Letters*. **19**: 3541–3545.

21. Peitsch MC (1996) ProMod and Swiss-Model: Internet-based tools for automated comparative protein modeling. *Biochem. Soc. Trans.*,**24**: 274–279.

22. http//www.seanet.com/ mthompson/Arguslab.

23. Morris GM, Huey R, Lindstrom W, Sanner MF, Belew RK, et al. (2009) Goodsell, D.S.; Olson, A.J. Autodock4 and AutoDockTools4: automated docking with selective receptor flexibility. *J. Comput. Chem.*, **162**: 785–791.

24. Lindahl E, Hess B, Spoel D (2001) GROMACS 3.0: A Package for Molecular Simulation and Trajectory Analysis. *J. Mol. Model.*, 7: 306-307.

25. Hess B, Bekker H, Berendsen HJC, Fraaije JGEM (1997) LINCS: A Linear Constraint Solver for Molecular Simulations. *J. Comput. Chem.*, **18**: 1463-1472.

26. Berendsen HJC, Postma JPM, van Gunsteren WF,Dinola A, Haak JR (1984) Molecular Dynamics with Coupling to an External Bath. *J. Chem. Phys.*, **81**: 3684-3690.

27. Morris GM, Goodsell DS, Halliday RS, Huey R, Hart WE, et al. (1998) Automated Docking Using a Lamarckian Genetic Algorithm and Empirical Binding Free Energy Function. *J. Comput. Chem.*, **19**: 1639-1662.

28. Molegro Molecular Viewer (MMV), **2008**. 1.0, Molegro, Denmark.

29. ChemAxon. MarvinSketch 4.1.8. **2007**. ChemAxonKft. Budapest, Hungary.

30. Discovery Studio 2.5 (2009) Accelrys Inc.: San Diego, CA, USA,